

Residual microstructure of a shaped-charge jet fragment

A. C. GUREVITCH, L. E. MURR, W. W. FISHER, S. K. VARMA, A. H. ADVANI
Department of Metallurgical and Materials Engineering, The University of Texas at El Paso, El Paso, TX 79968, USA

L. ZERNOW
Zernow Technical Services, Inc., San Dimas, CA 91773, USA

A recovered copper shaped-charge jet fragment has been built up by copper electrodeposition for the first time to allow it to be systematically sectioned and polished for detailed observations by optical and electron microscopy. The residual jet fragment microstructure was observed to have a recrystallized grain structure and dislocation substructures similar to those in the undeformed copper shaped charge liner cone. However, the average grain size in the recrystallized jet fragment was 15 μm compared to 45 μm for the liner. More significantly, however, SEM examination near the tips (or ends) of the jet fragment exhibited voids and coalesced void tunnels elongated axially within the fragment geometry, which are believed to have resulted during jet elongation and breakup by diffusion and viscous growth at high strain and strain rate. The observation of additional porosity in the interior of the jet fragment is supported by the lack of any similar observations in the surrounding and supporting (built up) copper electrodeposit.

1. Introduction

The development of the shaped charge over the last 50 years has provided unique applications both commercial and military. As an armour penetrator, a copper jet about 1.5 mm diameter, 0.5 m long, and travelling at near 10 km s^{-1} can make a 2 cm diameter hole in 1 m of mild steel. This remarkable phenomenon, in which a high explosive deforms and collapses a conical metal liner to form an elongating jet of the liner metal (illustrated schematically in Fig. 1), also represents one of the most severe examples of plastic deformation where strains vary from 500% to more than 1000% at strain rates between 10^4 and 10^7 s^{-1} !

Grace [1] has recently reviewed the principal features of the shaped charge in terms of the liner deformation stages, liner collapse and jet formation, and jet elongation and particulation (or fragmentation) (Fig. 1). In contrast to Fig. 1, Fig. 2 illustrates a shaped

charge undergoing explosive detonation. The deformation stages denoted in Fig. 2 involve the explosive shock loading of the liner metal (1) (at peak pressures between about 30 and 50 GPa), the liner collapse (2), pressurization and release at the so-called stagnation region (3) (where the pressure can reach peak values near 100 GPa, the elongation (or stretching) of the metal jet (4), and the jet particulation or breakup (5).

In conventional (military) shaped charges, such as the BRL (Ballistic Research Laboratory) 81 mm copper shaped charge, the shock loading of the liner occurs at strains of less than 10% and at a strain rate near 10^8 s^{-1} . The shock pressure is about 45 GPa and the shock temperature reaches 155°C . The liner collapse involves strains which vary between 500% and

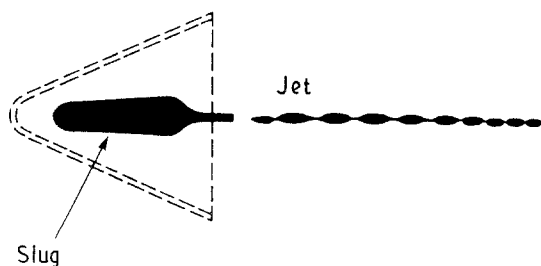


Figure 1 Schematic view of detonated shaped charge. A high explosive is detonated around a conical metal liner shown dotted, which collapses to form the slug and the elongating and fragmenting jet. The total cone angle is $\sim 61^\circ$.

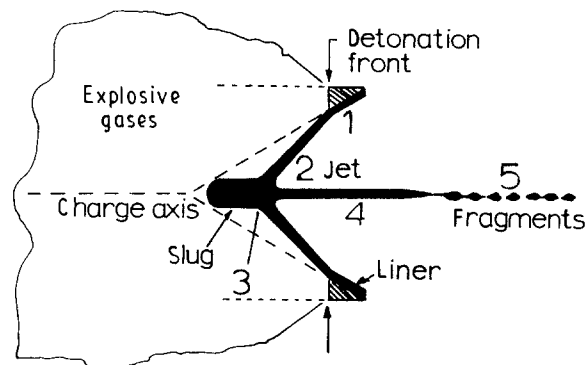


Figure 2 Schematic view of shaped charge undergoing explosive detonation. The deformation stages are denoted 1–5 and discussed in the text. (After Grace [1].)

1200% at a strain rate of 10^6 s^{-1} . At the stagnation point (3, Fig. 2), the peak pressure is $\sim 70 \text{ GPa}$ and the temperature is estimated to exceed $700 \text{ }^\circ\text{C}$ (see [2]). As the copper jet elongates, the strain exceeds 500% at a rate of about 10^4 s^{-1} , and the jet temperature is estimated to be about $400 \text{ }^\circ\text{C}$. Jet breakup occurs after about $100 \mu\text{s}$ from detonation at a strain of about 550%, and at a rate estimated to be 10^3 s^{-1} [1]. Zernow [3] was one of the first to conclude that the copper jet (including particulated components) remained in the solid state, while deforming plastically.

A knowledge of the physical state of the jet is crucial in determining its apparent ductility in relation to its breakup at the high rate it is stretched. As first shown by Plateau [4], when the length of a thin (fluid) cylinder exceeds a critical value, its surface energy is decreased by breaking (ideally) into spheres. Rayleigh [5] expanded this treatment into a theory of liquid jet instability which showed that a cylindrical liquid jet could continuously decrease its surface energy by breaking into droplets. Nichols and Mullins [6] extended this concept to solid rods within a solid body, and Miller and Lange [7] recently observed these features experimentally in polycrystalline (solid) fibres.

Recent estimates of the temperature (see [2]) at the stagnation region (3, Fig. 2) indicate that it does not exceed the melting point of copper, when computed on the basis of homogeneous heating. A few studies have been devoted to the recording of flash X-ray diffraction patterns of the stretching jets in copper and aluminium shaped charges [8–11]. Jamet and Charon [11] have shown that both copper and aluminium shaped-charge jets are in the solid state as originally postulated by Zernow [3], and aluminium exhibited a preferred orientation (texturing).

While there is rather compelling evidence that the grain structure of a copper liner has a marked influence on the stability of the corresponding copper shaped-charge jet, and the overall performance of the jet (especially armour penetration) and the shaped charge [12], there has been neither a systematic study of any metal liner or jet fragment microstructures (for example dislocation substructures), nor of their relationship.

In this investigation we examined the microstructure of a single recovered ETP copper jet fragment

and compared it with an undeformed ETP copper shaped-charge liner using a novel specimen preparation technique for transmission electron microscopy (TEM). Optical metallography and scanning electron microscopy (SEM) techniques were also used to provide a detailed overview of residual jet fragment microstructures and microstructure comparisons.

2. Experimental procedure

The jet particle used in this study was obtained by “soft” recovery of the jet from an ETP copper shaped-charge liner [13] using shaving cream in a long recovery cylinder positioned along the charge axis (shown in Fig. 2). However, the preparation of transverse sections from the jet fragment, in this study utilized a novel technique in which the recovered copper fragment was built up electrolytically [14] by wrapping the fragment with a small gauge copper wire and electrodepositing copper on to the wrapped fragment from a concentrated copper sulphate solution. Several “fragments” were fashioned from the liner cone and several similar size native copper fragments were used to practice this technique and optimize the electrodeposition parameters before the recovered jet fragment was successfully built up as shown in Fig. 3. This allowed the jet fragment to be readily sliced to prepare 3 mm discs (for TEM) which could be selectively electropolished to produce electron-transparent thin sections within the electrodeposited, encapsulated copper jet fragment. These features of jet fragment recovery and electrodeposit build-up are illustrated in Fig. 3 which also shows an ETP copper liner prior to explosive detonation.

Electron-transparent thin sections were also prepared from specimens cut and punched from the copper liner shown in Fig. 3 in order to compare relative microstructures observed by transmission electron microscopy. A Hitachi H-8000 analytical TEM operating at 200 kV was used to examine the electron-transparent thin sections sliced from various geometrical sectors within the liner and the electrodeposited jet fragment shown in Fig. 3.

Optical metallography was also performed on mating slices (and specimen surfaces) of both the recovered jet fragment and the undeformed conical liner

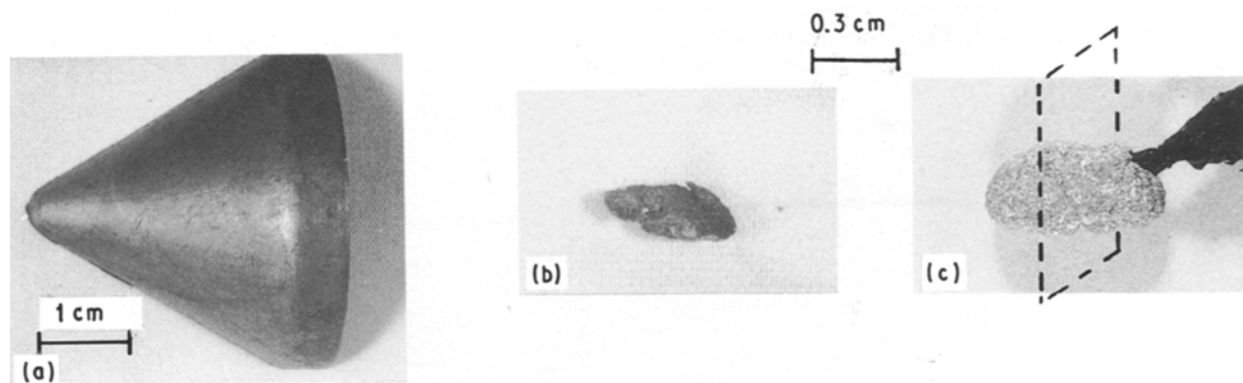


Figure 3 Experimental components in the shaped-charge regime. (a) Original, undetonated ETP copper liner (33 mm diameter, 2 mm wall). (b) Recovered ETP copper jet fragment from detonated shaped charge. (c) Copper electrodeposit on jet fragment in (b). The dotted plane represents the nature of transverse slicing of the built-up fragment.

(Fig. 3). A 50/50 nitric acid/water etch was employed for sample preparation prior to optical metallography. Scanning electron microscopy was also performed on the electro-thinned disc samples extracted from the jet fragment, as well as on other specimens.

3. Results and discussion

Fig. 4 illustrates the electropolishing [14] of a transverse section from the jet fragment shown in Fig. 3c and shows an electron-transparent region near the centre of the “soft-recovered” copper jet fragment [13]. This region is essentially centred in the disc, which includes the built-up rim of electrodeposited copper. Fig. 5 shows some typical bright-field transmission electron micrographs in the electron-transparent regions of the larger hole shown in Fig. 4c. This microstructure (in Fig. 5) is characterized by annealing twins and a significant number of dislocations ($\sim 10^9 \text{ cm}^{-2}$) which are not arranged in cell structures, and include a high density of dislocation loops. The electron diffraction pattern shown in Fig. 5 and other patterns representing different orientations show no anomalies in the copper lattice parameter

($a = 0.36 \text{ nm}$) or deviations from the crystallographic features expected for deformed copper.

In contrast to the jet fragment in Fig. 5, the microstructure of the ETP copper conical liner (Fig. 3a) consisted of some dislocation cells and annealing twins and (twin boundaries) as shown in Fig. 6. These two regimes are shown for comparison in Fig. 7 which illustrates optical microscope views of the corresponding grain structures and grain sizes. The grain size of the copper jet fragment is observed to be reduced from that of the liner by a factor of approximately 3 (from $45 \mu\text{m}$ to $15 \mu\text{m}$). However, the centre of the jet fragment exhibited some anomalously smaller grain sizes as a consequence of the jet formation as shown in Fig. 2. Zernow [13] has, in fact, observed a “central hole” in some copper jet fragments. In this region, grain sizes near $1 \mu\text{m}$ have been observed. Consequently, this average grain-size reduction, coupled with variations in residual microstructure (particularly dislocation structures) implicit in Figs 5 and 6, may be indicative of dynamic recrystallization in the jet fragment.

When the end sections of the recovered jet fragment were electropolished and examined in the SEM, a great deal of porosity was observed similar to that previously reported by Zernow [13]. Continued mechanical polishing and etching revealed this porosity to be a prominent feature of the jet fragment microstructure. The extensive nature of this porosity and the connectedness of voids within the jet fragment are illustrated in the sequence of SEM views shown in Fig. 8. The enlarged views in Fig. 8 show porous (void) tunnels extending from the electroetched surface areas. Of particular interest is the large tunnel surrounded by a region showing a refined grain structure and an interfacial crack delineating this grain-refined regime. The implications here seem to be that the porosity resulted by some combination of local mass transport and viscous void growth and coalescence, especially at the ends of the fragment where necking and fracture occurred.

Voids and porosity in a recovered shaped charge jet fragment were recently discussed for the first time by Zernow [13] and Zernow and Lowry [2] where evidence of elongated tunnel-like holes were seen in their SEM observations at the particle ends where they “necked” and separated from adjacent particles during jet breakup. However, their observations of microporosity in the particle interiors away from the ends were considered tentative and possibly due, in part, to artefacts arising from the mechanical polishing process, the presence of oxides in the ETP copper, or chemical etching effects. The present observations, however, provide stronger evidence for porosity in the jet fragment interior because the surrounding copper electrodeposit has been subjected simultaneously to identical mechanical and chemical processing, and this region exhibits no porosity or void microstructures as shown in Fig. 9.

Fig. 9 summarizes the observations of voids within the shaped-charge jet fragment by showing low-magnification optical microscope views of longitudinal (Fig. 9a) and transverse (Fig. 9b) sections from the jet fragment shown in Fig. 3c. Fig. 9c and d illustrate

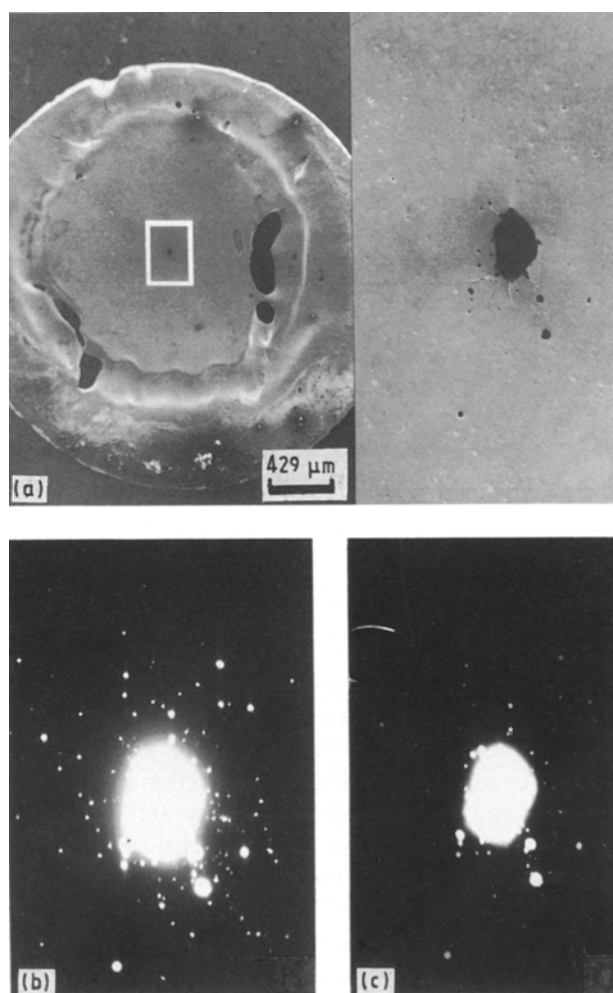


Figure 4 Slicing, 3 mm disc punching, and preparation of electron transparent thin sections in transverse sections cut from the recovered copper jet fragment in Fig. 3c. (a) SEM views of the electropolished disc. (b) TEM view of the central, thinned region in (a). (c) Over exposure of (b) showing fiducial details in (a).

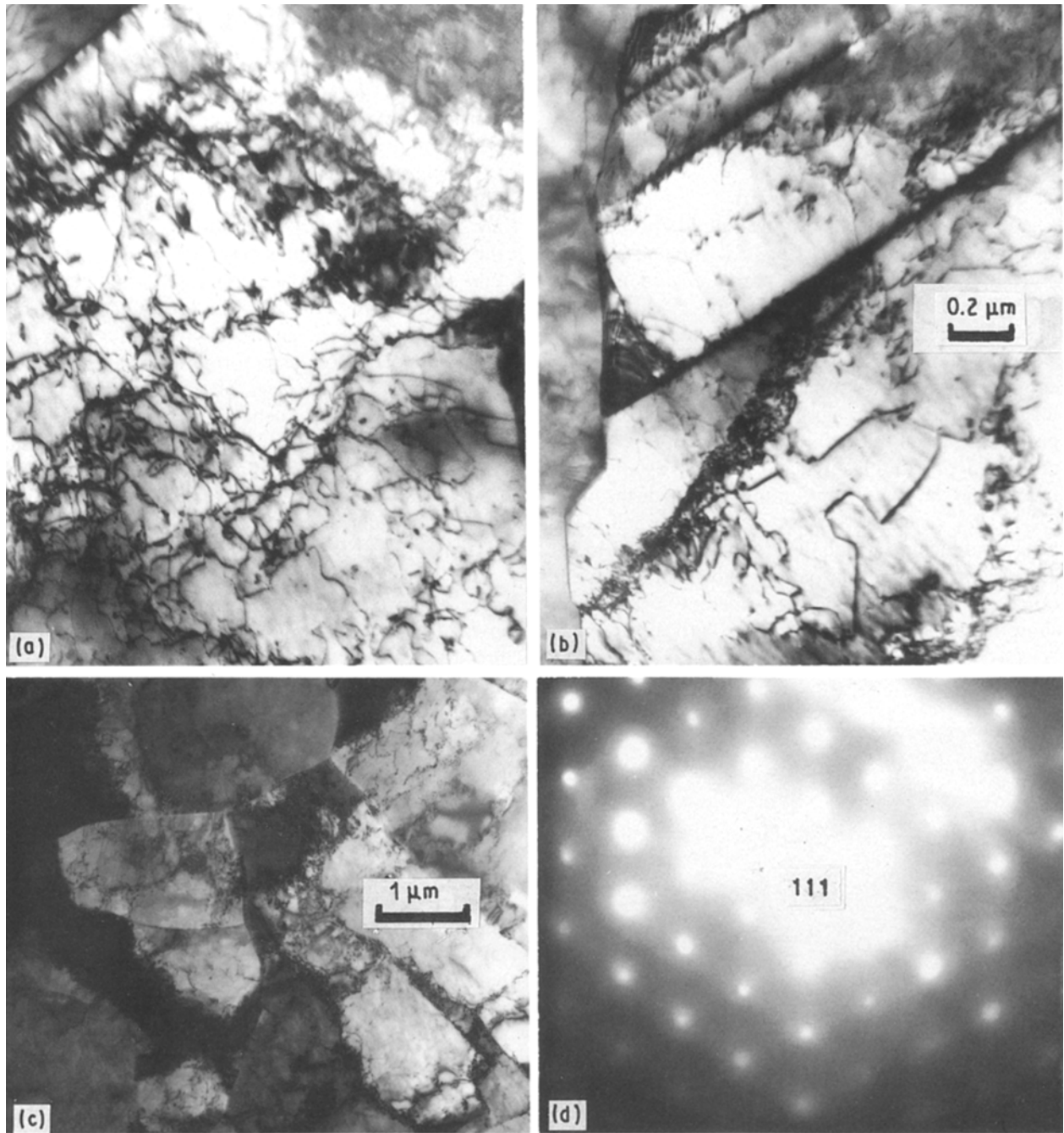


Figure 5(a-c) Dislocations and annealing twins representing apparent recrystallization microstructures in the recovered ETP copper shaped-charge jet fragment. (d) Selected-area electron diffraction pattern illustrating the crystallographic nature of the region shown in (c).

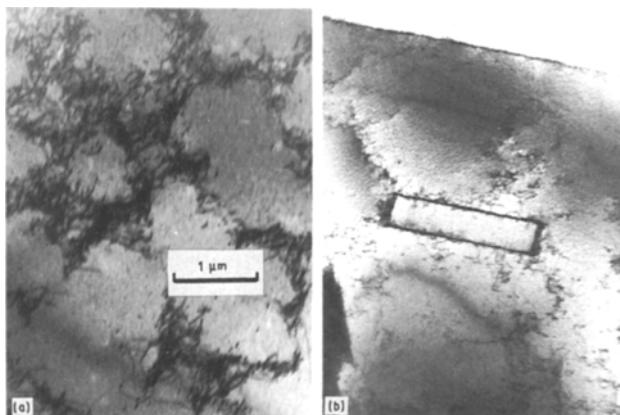


Figure 6(a, b) Dislocation cells and annealing twin structures in the undetonated copper liner cone.

schematically these two views and the geometry of voids observed in Fig. 9a and 9b. Fig. 9a and b show the extent of porosity which has been estimated to be about 7% from these views (Fig. 9b) and the SEM views (as in Fig. 8). It should be noted in Fig. 9a that the etching was allowed to exaggerate the microstructure, especially the voids. Consequently, this is representative of the void geometry but not their proportion. In addition, this measurement is not necessarily representative of the entire fragment, and applies only to the section examined. Indeed, it can be observed from Fig. 9a that the high porosity measured occurs at the end of the fragment where the voids are also elongated. Consequently, as implicit in the sketch of Fig. 9d, the void density will be less in the particle centre. The hypothesis of high porosity in the interior

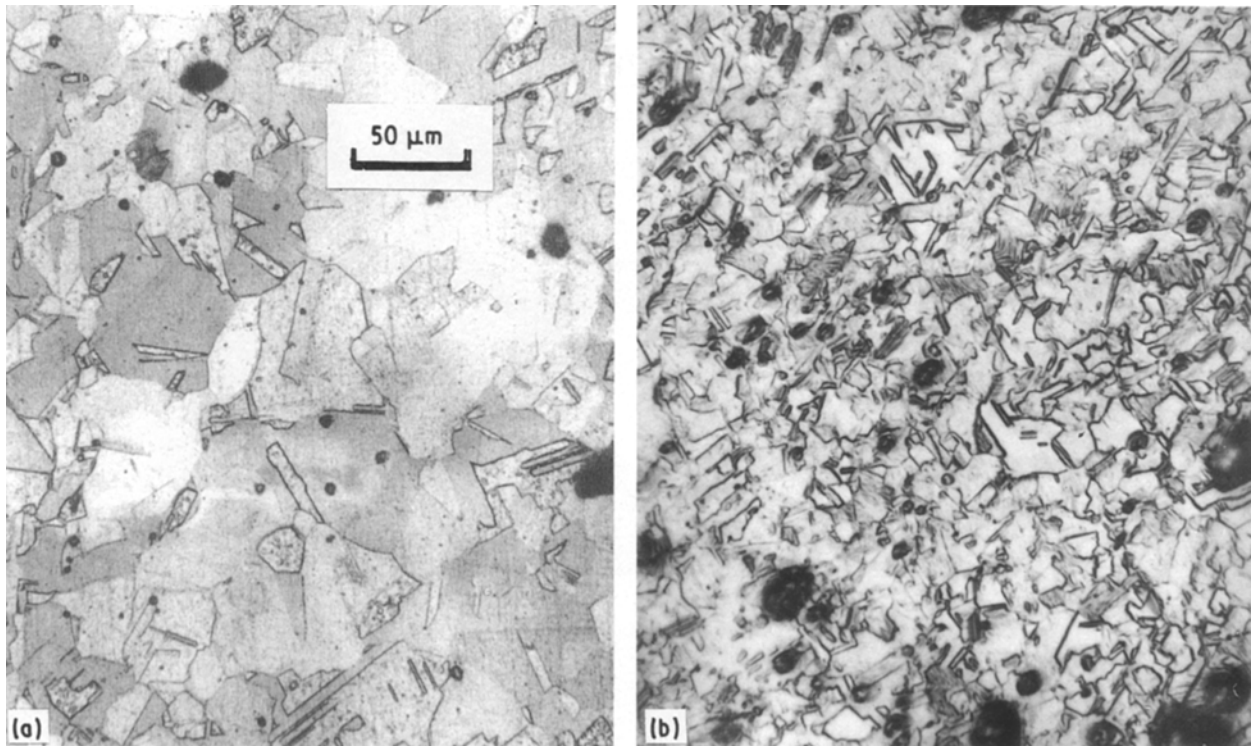


Figure 7 Optical (metallographic) views of grain structure in ETP copper liner (longitudinal) section (a) and longitudinal ETP copper jet fragment section (b) for comparison. The region of the fragment shown is near the outside surface edge, away from the jet fragment central axis. (See Fig. 9(c) for orientation features.)

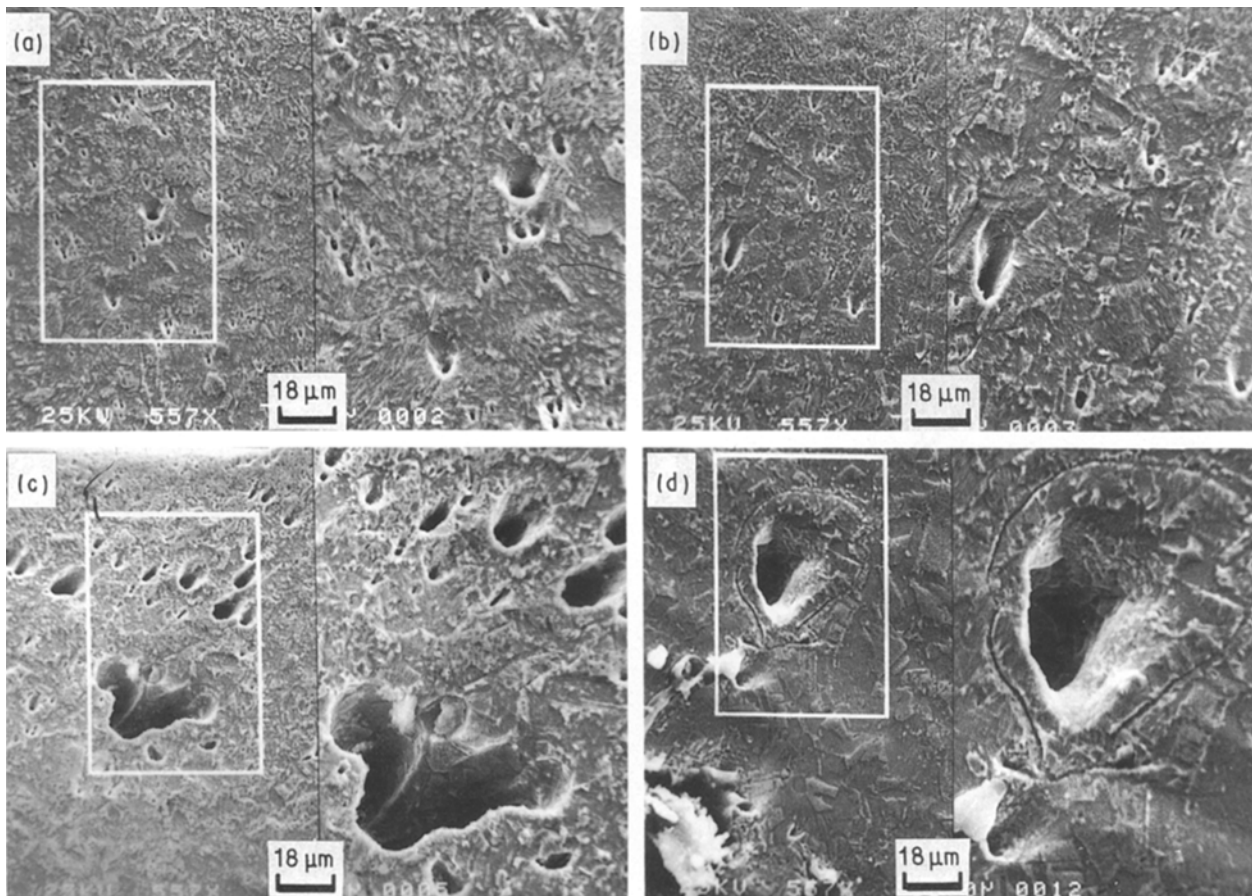


Figure 8(a-d) Examples of porosity and continuous, interconnected porosity creating void or pore tunnels at various locations within the jet fragment as shown in Fig. 9a (1-4, respectively).

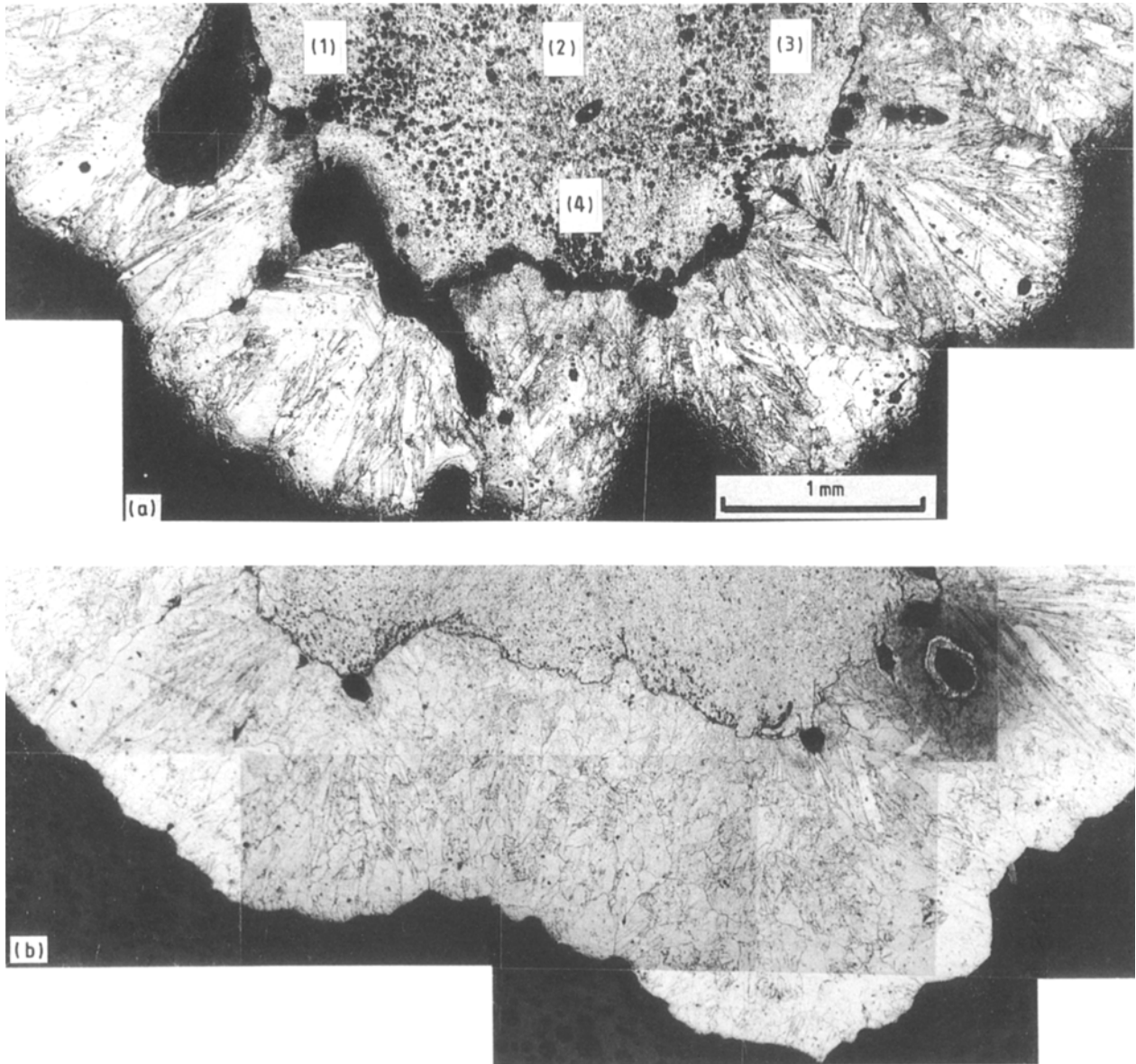
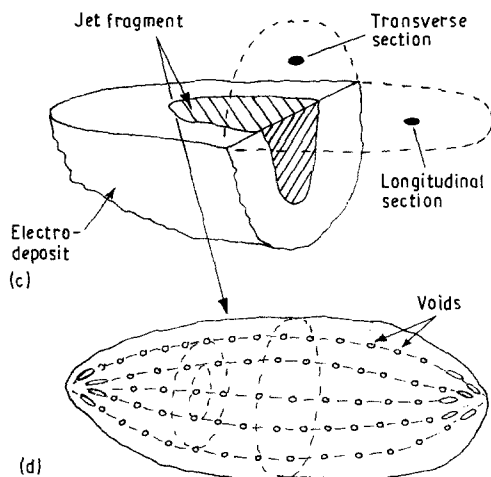


Figure 9 Composition of optical micrographs showing longitudinal (a) and transverse (b) section views of the built-up shaped-charge jet fragment in Fig. 3c. The electrodeposited copper is readily distinguished from the fragment. (c) A schematic of these views in relation to the sectioned jet fragment; (d) the geometries of the void structure observed in (a) and (b).



of the jet particle is not supported by X-ray densitometry measurements.

The void geometry implicit in Fig. 9d and reconstructed schematically from the microscopic views shown in Fig. 9a and b provides some indication of the jet formation and particulation. Because of the ellipsoidal void configurations observed (Fig. 9d), it might

be postulated that the voids formed during jet elongation, and the ellipsoidal geometry results because the fragments are stretching at necking instabilities (where breakup occurs) which creates ellipsoidal overall jet fragment shapes. At the high rates of plastic straining which characterize the jet, the voids are nucleated and coalesced by diffusion and viscous growth [15–18]. Curran *et al.* [18] have, in fact, illustrated spherical voids having an appearance similar to those in Fig. 9a and b in copper impact specimens.

While there is some evidence of dynamic recrystallization because of the grain-size reduction in the jet fragment as compared to the undeformed liner, the average grain size of the jet fragment away from the centre axis (Fig. 7) is more than a factor of 100 larger than the grain size calculated by Chokshi and Meyers [19] to be associated with dynamic recrystallization

for strain rates near 10^4 s^{-1} . In addition, the grain size observed in the jet fragment examined in this research programme is considerably larger than that observed in a copper shaped-charge slug (see Fig. 2) examined by Chokshi and Meyers [19]. Consequently, we cannot confirm the prospects for superplasticity at high strain rates alluded to in the recent work of Chokshi and Meyers [19]. Furthermore, the considerably different microstructural features they see for a copper shaped-charge slug are indicative of the considerable differences in the strain and strain-rate history to which the material in the slug is subjected, as contrasted with the material in the jet (see Fig. 2). In addition, we would expect the ETP copper to contain some oxide inclusions which would contribute to void formation. We have not seen a great deal of convincing evidence of such inclusions in the TEM analysis.

Because of the prominence the voids assume in the residual copper shaped-charge jet fragment microstructure, their formation and coalescence may play a particularly important role in the jet formation and instabilities leading to breakup and fragmentation. If this is true, then the addition of impurities or inclusions to the liner may have a significant influence on void formation and on the jet formation. Indeed, Tvergaard [20] has described the influence of voids on shear-band instabilities, and while we have not seen any evidence of shear bands in the recovered copper jet fragment, there are similarities between the plastic strains and heating which occur in the elongating jet, and shear instabilities.

While Fig. 9, as a consequence of the method of specimen preparation, does not show a prominent central hole in the jet fragment recently illustrated by Zernow [13] and Zernow and Lowry [2], the observations of porosity shown schematically in Fig. 9d are consistent with those reported previously by them [2], especially in regard to a contribution of the porosity to the necking and fracture of individual particles. There is evidence, as shown in Fig. 9a, that a microcrystalline area (having grain sizes smaller than the average of $15 \mu\text{m}$ observed away from the particle axis) circumscribing a central region of the jet fragment exists similar to that described previously where a central hole was observed as a consequence of the concentric formation of the jet from the inner wall movement of the cone along the charge axis shown in Fig. 2 [2, 13].

4. Conclusion

A novel recovery scheme and a novel method for building up a small fragment has allowed a copper shaped-charge jet fragment to be systematically examined by optical, scanning electron, and transmission electron microscopy. In addition, the recovered ETP jet fragment microstructure has been compared with the microstructure for an undeformed ETP copper liner in order to continue a detailed assessment of the possible role liner microstructure may have on the formation and stability of the jet which forms in an explosively detonating shaped charge. The most significant microstructural observation in the recovered

copper jet fragment was the occurrence of extensive void formation and coalescence into long "tunnels". Dislocation structures in the recovered fragment resembled those in the undeformed, starting copper liner material except that the grain size of the fragment was reduced from that of the liner, indicating some dynamic recrystallization occurring simultaneously with void nucleation, growth, and coalescence. The fact that porosity and similar features were not observed in the surrounding built-up electrodeposit, unambiguously attests to these microstructural observations.

Because of the enormous strain and high rate of deformation, the void growth probably occurs by diffusion and viscous flow. To the extent that void formation may be an important feature of shaped-charge jet formation and stability, impurities in the liner may have a significant influence because void nucleation and growth would be significantly influenced. The microstructures of the starting liner, the residual slug, and the jet particles, are known to be considerably different. A more detailed analysis and comparison is indeed warranted, and is underway in continuing studies.

Acknowledgements

This research was supported in part by Zernow Technical Services Inc. (Contract ZSC-90-002(4172), funded under Zernow Technical Services Prime Contract N60921-89-C-0172; jointly by the US Navy, US Army, and DARPA), the Phelps Dodge Foundation (through the Phelps Dodge Scholarship Program (A.G.)), and a Mr and Mrs MacIntosh Murchison Endowed Chair (L.E.M).

References

1. F. I. GRACE in "Shock-Wave and High-Strain-Rate Phenomena in Materials", edited by L. E. Murr, M. A. Meyers and K. P. Staudhammer (Marcel Dekker, New York, 1992) p. 493.
2. L. ZERNOW and L. LOWRY, in "Shock-Wave and High Strain Rate Phenomena in Materials", edited by M. A. Meyers, L. E. Murr, K. P. Staudhammer (Marcel Dekker, New York, 1992) Ch. 46.
3. L. ZERNOW, PhD dissertation, Johns Hopkins University, MD, USA (1953).
4. J. PLATEAU, "Statique experimentale et theoretique des liquides soumis aux seules forces moleculaires" (Paris, 1873).
5. J. S. W. RAYLEIGH, "Theory of Sound", Vol. II (Dover, New York, 1945).
6. F. A. NICHOLS and W. W. MULLINS, *J. Appl. Phys.* **36** (1965) 1826.
7. K. T. MILLER and F. F. LANGE, *Acta Metall.* **37** (1989) 1343.
8. R. E. GREEN Jnr, *Rev. Sci. Instrum.* **46** (1975) 1257.
9. F. JAMET and G. THOMER, *C. R. Acad. Sci. (Paris)* **B279** (1974) 501.
10. F. JAMET, "Investigation of Shaped Charge Jets Using Flash X-Ray Diffraction", 8th Symposium on Ballistics, Orlando, FL, October 1984.
11. F. JAMET and R. CHARON, "A flash X-ray diffraction system for shaped charge jets analysis", Report (0211/86) Franco-German Research Institute, Saint-Louis, France, 15 May, 1986.
12. M. L. DUFFY and S. K. GOLASKI, "Effect of Liner Grain Size on Shaped Charge Jet Performance and Characteristics", Technical Report BRL-TR-2800, US Army Ballistic Research Laboratory, Aberdeen Proving Ground, MD, 7 April, 1987.

13. L. ZERNOW, "Metallurgical, XRD, and SEM Studies of Individual Shaped Charge Jet Particles Captured by Soft Recovery", International Conference on Ballistics, Nanjing, China, October 1988 (Chinese Academy of Science).
14. L. E. MURR, "Electron and Ion Microscopy and Microanalysis", 2nd Edn (Marcel Dekker, New York, 1991).
15. L. SEAMAN, D. R. CURRAN and D. A. SHOCKEY, *J. Appl. Phys.* **47** (1976) 4814.
16. L. SEAMAN, D. R. CURRAN and R. C. CREWDSON, *ibid.* **49** (1978) 5221.
17. J. R. RICE and D. M. TRACEY, *J. Mech. Phys. Solids* **17** (1969) 202.
18. D. R. CURRAN, L. SEAMAN and D. A. SHOCKEY, "Shock Wave and High-Strain-Rate Phenomena in Metals", edited by M. A. Meyers and L. E. Murr (Plenum Press, New York, 1981) Ch. 9, p. 129.
19. A. H. CHOKSHI and M. A. MEYERS, *Scripta Metall. Mater.* **24** (1990) 605.
20. V. TVERGAARD, "Influence of Voids on Shear Band Instabilities under Plane Strain Conditions", Report no. 159, Technical University of Denmark, June, 1979.

*Received 27 February
and accepted 8 October 1992*